ORIGINAL ARTICLE

Feasibility study of microplastic biodegradation in effluents from South Tehran WWTP after quantitative and qualitative measurement of the particles

Somayeh Shirazi[1] · Roya Mafigholami[1] · Hamid Moghimi[2] · Seyed Mehdi Borghei[3]

Abstract

Microplastics are currently known to be among the most detrimental environmental. The research on ways to counteract these pollutions and the use of microorganisms for the biological decomposition of various plastic polymers have evolved over the recent years. In this regard, the present study collected effluents from the southern Tehran treatment plant and separated and counted the microplastics present in them, it was found that the least number of microplastics was found in the samples of the summer season and the highest number of microplastics was found in the samples of the spring season. In these samples, particles could be identified in three forms: fiber, fragment, and film, which revealed that the most frequently observed microplastics were polypropylene and then polyethylene. These microplastics combine with the microbes in the culture medium. Three microbial colonies that survived were then separated and identified, which revealed that these bacteria included *Achromobacter denitrificans* (sample B), *Bacillus amyloliquefaciens* (sample C), and *Pseudomonas aestusnigri* (sample E). Moreover, the decomposition of polypropylene and polyethylene microplastics exposed to isolates was examined through various methods. Results of cellular gravity examination indicated that the average weight reduction in the PP sample exposed to B and E bacterial isolates was 38.2% and 58.9%, respectively. In the SEM images, the surface of the polymers of these two isolates is more uneven. Moreover, the mean cellular weight reduction for PE-based microplastic exposed to isolate C was 13.3%, the results of FT-IR tests showed that the peaks in the samples exposed to strains B and E were accompanied by changes compared to the control sample (G). The results of the TGA test also confirm the greater effectiveness of the bacterial strain E. It was based on the polymer structure. In the Raman spectrum of sample E, some peaks have been removed and new peaks with other shifts have appeared in their place. Results were confirmed by carbon dioxide emission tests and the produced protein amount.

Keywords Biologic treatment · Effluents · Microplastic · Polyethylene · Polypropylene

✉ Roya Mafigholami
r.mafigholami@wtiau.ac.ir

Somayeh Shirazi
kiaradvosuq91@gmail.com

Hamid Moghimi
hmoghimi@ut.ac.ir

Seyed Mehdi Borghei
mborghei@sharif.edu

[1] Department of Environmental Science and Engineering, Islamic Azad University, West Tehran Branch, Tehran, Iran

[2] Department of Microbiology, School of Biology, Collage of Sciences, University of Tehran, Enghelab St., PO Box 6455-14155, Tehran, Iran

[3] Faculty of Chemical and Petroleum Engineering, Sharif University of Technology, Azadi St., Tehran, Iran

Introduction

As the main component of waste, plastics are made out of polymer monomers and are among the newest and most serious environmental challenges (Halden 2010). Microplastics with dimensions smaller than 5 mm are widely spread across the world. These microplastics can transmit contaminants to humans and other living organisms through food chains and leave adverse impacts on the health of the environment and living organisms (Żwierełło et al. 2020; Burns and Boxall 2018). On the other hand, they can carry microorganisms and species invading ecosystems (North and Halden 2013). Phthalates and hydrocarbon aromatic rings are among the prominent examples of microplastics present in industrial effluents, surface water and sediments, compost leachates, and land-fills (Żwierełło et al. 2020; Chen and Patel 2012). Studies suggest that when decomposed into nanoparticles, these microplastics can infiltrate the biofilm and produce inactive oxygen compounds that leave acute inhibitory influences on biodegradation key enzymes, the microbial community, and final products (Auta et al. 2017; Horton and Dixon 2018). Moreover, microplastics can easily absorb and carry organic contaminants, metals, and pathogens due to their extremely hydrophobic surface (Issac and Kandasubramanian 2021). Considering that various additives such as Phthalates are used in plastic production, the combination of these micro-contaminants and the additives exacerbates the adverse impacts of microplastics on sewage sludge and wastewater (Prata 2018). Given the widespread applications of plastics in daily life and their negative impacts on the health of living organisms and ecosystems, solutions must be devised to turn these structures into decomposable and eco-friendly structures, among which biodegradation is one method (Elahi et al. 2021; Susanti et al. 2020).

The use of microorganisms as cellular biocatalysts prevents the exhausting production and purification stages in the enzyme production process and enables repeated use in sequential reactions (Fukuda et al. 2008; Bräuti-gam et al. 2009). Many studies have been conducted in this respect to use bacterial isolates to decompose various microplastics. Yoshida et al. (2016) isolated a new bacterium called Ideonella sakaiensis 201-F6 from the outputs of a bottle recycling center and demonstrated that it could use polyethylene-terephthalate-based (PET) microplastic as its main carbon and energy resource and turn PET into two eco-friendly monomers. In another study, Gao and Sun (2021) used a set of marine bacteria to decompose the structure of PET and PE polymers. They used sequencing methods and 16SrRNA absolute quantitative culture in this study to obtain the corresponding frequency and

achieved pure three-isolate bacterial cultures that could decompose plastics.

In the following article, in addition to the study of microplastics present in effluents from South Tehran WWTP, for the first time, the ratio of nanoplastic particles to microplastics in the sewage treatment plant was calculated, because many microplastic particles can be received along the path to the house and it was also in the stream until the exit, they are crushed and at the time of counting—if the nano size is not taken into account—it is ignored or in the announcement of the efficiency of the treatment plant systems in removing these particles, and also in this research, the quantitative and qualitative monitoring of existing microplastics, for the first time, to feasibility Microbial degradation of the types of polymers identified by the microbial strains present in the natural environment of wastewater. Using the microbial strain of the natural environment will definitely have more practical conditions in the future use of this research.

The identified microplastics with the highest number in the wastewater were combined with the microbes present in the wastewater in the culture medium, and while identifying the microbial colonies, the destruction of the chemical structure of the microplastics in the presence of these microbes was investigated.

Materials and methods

Sampling and sample preparation

Sampling was performed from the effluents of the South Tehran urban wastewater treatment plant over a year to prepare the effluent solution. In each month, 4 samples of 1 L were taken from the effluent of the treatment plant (48 L in total). For sampling, closed glass containers with a volume of 1 L are used. A solution containing 0.05 iron ion and 6 ml 98% sulfuric acid was used based on the recommendation of the American National Oceanic and Atmospheric Administration to ensure the complete dissolution of the organic compounds in the effluent. 0.45 microns cellulose nitrate membrane filters were used to filter the solution. Furthermore, weight separation was used to separate the non-plastic materials such as silt and clay particles. Characterization and counting the microplastics found through this method revealed that polyethylene and polypropylene were the most abundant microplastics. Thus, these two microplastics were synthetically prepared and used for further microplastic examinations. After adding these materials, the samples were placed on a magnetic shaker for 30 min at a temperature of 60° (N. Marine Debris Program 2015). The temperature of more than 60° can destroy the structure of some polymers such as PET. After this stage, the samples were kept at room temperature for 24 h so that the digestion

process can be done well. Cellulose nitrate membrane filters with a size of 0.45 micron were used for filtering the solution. Also, weight separation method was used to separate non-plastic materials such as clay and silt particles. For this separation, zinc chloride solution with a concentration of 5.5 mol (1.7 g/cm^3) was used to obtain the maximum amount of microplastics (95%). 20 ml centrifuge tubes were filled with this solution and the filters were immersed in it. Then put the tubes in the ultrasonic bath for 10 min to separate all the materials from the filter. The ultrasonic power was set to 60%. Then the centrifuge is used for 5 min at 4000 rpm to separate the non-plastic materials and float the microplastics. Then filter the floating particles again to ensure that the particles on the filter are microplastic. Then, the obtained filters were placed in an oven at a temperature of 60 degrees for 60 min to dry, and then they were placed in a desiccator to prepare for Raman and microscopic analysis.

Preparation of microplastics

Preparation for polymer identification

In order to prepare microplastics, pellet-type plastics with a diameter of 3–4 mm were prepared. Then, in order to crush them, first using nitrogen, their temperature reached 196 degrees Celsius, and then it was ground using a centrifugal grinder. Before photographing with SEM, a layer of gold was sputtered on the samples to establish the conductivity of the samples. The images were taken with a voltage of 10 kV and a detector distance of 9 mm. Identification of microplastics is done by recognizing their appearance. These particles can be fibers with a thin and long appearance or fragments with a smooth or broken appearance or sphere-shaped. Also, film particles with a flat and thin appearance can exist. During the scanning process, the number, size and size of micro-nanoplastics were recorded using ImageJ software. Micro- and nanoplastics were divided into 6 categories in terms of dimensions (0.2–1, 1–5, 5–10, 10–50, 50–100 and above 100 μm). Next, 20 microplastics were separated from the filter and placed on copper glue and prepared for spectroscopic analysis. The laser wavelength of the Raman device was 785 nm. The obtained spectra were compared with the database of infrared and Raman spectra (IRUG) and polymers were identified.

Preparation of samples for microbial analysis

Microplastics were incubated by mineral salt medium (MSM). During this process, most microorganisms have found the ability to break down into microplastics. In this regard, 1% w/v of microplastics incubated in MSM was placed in the following medium:

1 g of NH_4Cl, 3 g of KH_2PO_4, 7 g of Na_2HPO_4, 0.25 g of $MgSO_4$, 0.5 g of NaCl and 1 mL of trace elements solution (40 mg L^{-1} of $CuSO_4.5 H_2O$, 0.2 mg L^{-1} of $FeCl_3$, 0.4 mg L^{-1} of $ZnCl_2$, 0.4 mg L^{-1} of $MnSO_4$, 0.2 mg L^{-1} $(NH_4)6MO_7O_{24}.7 H_2O$, and 0.5 mg L^{-1} H_3BO_3) per liter of distilled water; pH 7 ± 0.05.

Effluent was added to the medium mentioned above, and the solution was stirred at 30 °C for a month at 150 rpm. After a month, 1 mm of suspension was added to the medium again and the aforementioned was repeated three times. Subsequently, 100 μl was drawn from each Erlenmeyer flask and cultivated on a nutrient agar medium plate, and the microplastic decomposing microbial isolates were separated and stored in the fridge for further experiments.

Examination of microplastic decomposition extent

The cell dry weight

Bacterial isolate growth kinetic obtained based on the dry weight in a saline-based culture medium containing 1000 mg microplastics can be a basis for this substance's amount of consumption by the inoculated bacteria. Following the bacteria inoculation into the saline-based culture medium containing 1000 mg microplastics and the pre-culture period, incubation was performed doe 30 days at 28 °C with a shaker speed of 150 rpm. After this stage was completed, the contents of the flasks were centrifuged at 8000 rpm. The obtained supernatant was disposed of. At the nest stage, the sediments were stored at 65 °C for 48 h. The dry weight of the sediments was obtained after the end of this time and the evaporation of the interstitial water. Equation 1 was used to calculate the weight loss.

$$\% \text{ Weight loss} = \left(\frac{W0 - W}{W0} \right) \times 100 \qquad (1)$$

where $W0$ is the initial weight (g), and W is the remaining weight of the microplastics. The measurements of this experiment were performed in three iterations.

Examining microplastic decomposition extent based on carbon dioxide content

The number of microbial activities can be used to measure the decomposability of these microplastics. Microbial activity can be determined through respiration. The carbon dioxide produced by the organisms is usually entrapped in a sodium hydroxide solution to determine respiration through conductometry or titration. In a titration, the amount of the hydroxide that has not participated in the interaction is measured. For this purpose, microplastics with a concentration of 1000 mg/l were first inoculated into the medium culture, and oxygenation was then performed in the glasses so that

all the carbon dioxide was discharged from the medium. The inoculated bacteria were incubated at 28 °C and shaker speed of 150 rpm for 21 days after being transferred from the pre-culture to the main culture medium. After the incubation ended, oxygen was injected into the glasses again so that all the carbon dioxide generated throughout the decomposition process was trapped in a 0.2 M KOH solution. 1 ml of barium chloride solution (M0.5) and three drops of 1% phenolphthalein reagent were then added. The residual hydroxide potassium was titrated with standard HCL solution (0.1 M). The amount of the carbon dioxide generated by the end of day 21 was calculated based on the HCL consumed in titration as Eq. 2 demonstrates (Cerqueira et al. 2013).

$$\left(V_{B-}V_A\right) \times \left(M_{CO_2}\right) \times M_{HCl} \times C_F \quad (2)$$

where V_B volume of HCL consumed in control, V_A volume of HCL consumed in the sample, C_F: M_{HCl}/M_{KOH}.

Measuring the extent of microplastic decomposition based on the amount of generated protein

Measuring the amount of protein generated as a result of microplastic decomposition by the obtained isolates can indirectly reveal the isolate's capability in plastic decomposition. The method proposed by Lowry et al. (1951) was used to measure the generated protein. Specific concentrations of bovine serum albumin ranging from 0.1 mg/ml to 1 mg-ml in deionized water were prepared and their light absorption was determined based on the method proposed by the mentioned researchers to obtain the standard curve of protein measurement.

Molecular identification of the obtained strains

The 16 s rRNA fragment was amplified and sequenced using the PCR method to perform molecular identification. The desired and its sequence were then compared to the sequences available on NCBI databases and the unknown organisms were identified based on their percentage of similarity to the identified genes. The method proposed by Sambrook and Russell (2006) was used for this purpose.

In short, to extract DNA through this method, the isolates of interest were first inoculated into a nutrient broth culture medium and incubated until proper biomass was reached. After washing and physical crushing through grounding the biomass frozen using liquid nitrogen, the cells were broken and the DNA was isolated using the phenol–chloroform extraction technique. The extracted DNA had to be amplified through PCR for molecular isolate identification. 27F and 1492R general primers were used to perform the PCR.

After performing the PCR, 1% agarose gel was used to perform horizontal electrophoresis seeking to ensure DNA sample purity and determine amplified fragment length (Sambrook and Russell 2006).

Identification methods

A Scanning Electron Microscopy (SEM) test was conducted using the FESEM-TESCAN MIRA3 model microscope with a voltage of 10 kV and detector distance of 9 mm. A layer of gold applied on the surface through magnetic sputtering was used to create conductivity. Thermogravimetric Analysis (TGA) was used to investigate the thermal properties of PE and PP polymers before and after exposure to bacteria. A TGA/SDTA 851 Metter Toledo was used under linear heating conditions to examine the thermal stability of samples. This analysis was performed in a nitrogen environment in the thermal range of 25–800 °C with a 10 °C increase in temperature per minute. Moreover, Raman and Fourier Transform Infrared (FTIR) spectroscopy were performed to examine the changes in chemical bonds of the samples before and after exposure to bacteria. Raman spectroscopy was conducted at the RS (100–4600) range using the Takram P50C0R10 device, and FTIR spectroscopy was performed by the Perkin Elmer, US device using KBr tablets in the 400–4000 cm^{-1} wavenumber range (Rizzarelli et al. 2016).

Results and discussion

What was obtained from the results of the seasons of the year, the number of samples was more than 3500 microplastics in every 1 wastewater sample (Table 1), which on

Table 1 The number of micro- and nanoplastic particles in different seasons

Season	Number of nano-plastics	Percentage nano-plastic	Number of micro-plastics	Percentage micro-plastics	Total micro nanoplastics
Spring	14,664	31/03	32,579	68/97	47,243
Fall	15,009	34/95	27,929	65/05	42,938
Summer	13,887	35/61	25,101	64/39	38,988
winter	14,847	37/30	24,956	62/7	39,803
Total	58,407	Average 34/72	110,565	Average 65/27	168,972

average was 47.48% fiber, 47.47% fragment and 5.05% film. Polypropylene was the most with 5 particles, followed by polyethylene with 4 particles.

After that, in the order of 3 cases of PET, PTFE, PA,PS, PBT, PVA and PU, only 1 case each and PVC, 2 cases were observed.

Molecular identification

After ensuring the purity of the extracted DNA, the PCR product was sent over to Macro Gene Co., South Korea. The sequences were compared to the sequences on the NCBI gene bank. In terms of sequence heterogeneity. Table 2 reports the isolates obtained from these examinations.

As Table 2 demonstrates, three isolates were identified which can result in changes in the structure of microplastics by altering their chemical structure and eventually contribute largely to the conversion of these structures to structures with a higher filtration potential. The impact of each strain on the chemical structure of polyethylene-based and polypropanol-based microplastics has been discussed in the following, and the strains have been compared to one another in terms of their impact on the chemical structure of microplastics. For this purpose, strain C has been used to decompose polypropylene-based microplastics, and strains B and E have been used to decompose polyethylene-based microplastics.

Characterization

SEM test was used in the present study to investigate the morphological and microstructural changes in the studied microplastics after exposure to the bacterial strains. Figure 1 demonstrates the resulting micrographs.

As Fig. 1 demonstrates, comparing the treated samples to control samples reveals that treating the samples with microbial strains B and E for three months resulted in a coarser polymer surface which can indicate that the bacteria invaded this microplastic surface during the process (blue arrow). Meanwhile, the polymer exposed to bacterial strain C maintained its smooth surface which can indicate the lower ability of this strain in polymer structure decomposition. Still, the cavities and fractures observed in sample C and a more uneven surface is thus observed in this sample compared to the control sample (red arrow). Moreover, various cavities,

Table 2 molecular identification of the obtained isolates

Isolate	Identified strain	Similarity (%)
B	*Achromobacter denitrificans*	99
C	*Bacillus amyloliquefaciens*	99
E	*Pseudomonas aestusnigri*	100

irregularities, and horizontal fractures are observed in the sample exposed to strain E which are more visible compared to the other microbial and control samples. This can be a sign of the greater impact of this strain on the chemical structure decomposition of microplastics compared to the other strains.

The impact of the various strains on the chemical structure of microplastic was examined using chemical characterization tests (FTIR and Raman), and the results were compared. Figure 2 demonstrates the results of Raman spectroscopy on PE and PP baseline samples before and after bacterial exposure.

In Fig. 2a, the peaks at Raman shifts 1059 cm^{-1}, 1079 cm^{-1}, and 1126 cm^{-1} are associated with the stretching vibrations of the C–C bonds (Rizzarelli et al. 2016). Furthermore, the peaks at Raman shifts 1166 cm^{-1} and 1293 cm^{-1} are associated with the rocking vibrations of CH_2 groups and twisting vibrations of the C–H bonds, respectively (Furukawa et al. 2006). The wagging vibration of CH_3 bonds at 1367 cm^{-1} also led to a peak (Visentin et al. 2006). The peaks at Raman shifts 1415 cm^{-1}, 1438 cm^{-1}, and 1459 cm^{-1} are also associated with the bending vibrations of CH_2 bonds. Figure 3a demonstrates that no change in the general polyethylene structure has been made after this polymer was exposed to microbial strain C, although the intensity of the peaks has declined. The reduced peak intensity could be due to the polymer chains breaking after exposure to this microbial strain. In other words, the microbe used in sample C only managed to break the polymer change but failed to form a new structure and has not changed the sample from its polyethylene state.

As Fig. 2b demonstrates, the peaks in Raman shifts 805 cm^{-1} and 1034 cm^{-1} were associated with the stretching vibrations of C–C bonds in the control sample (G) which was not exposed to bacteria (Rizzarelli et al. 2016). Moreover, the peaks on Raman shifts 837 cm^{-1} and 969 cm^{-1} were associated with the rocking vibrations of CH_3 groups (Rizzarelli et al. 2016; Jung et al. 2018). The peaks on Raman shifts 994 cm^{-1}, 1149 cm^{-1}, and 1164 cm^{-1} were associated with the bending vibrations of the Ch_2 bonds (Cerqueira et al. 2013; Lowry et al. 1951; Sambrook and Russell 2006; Rizzarelli et al. 2016). The wagging vibrations of C–H bonds, the twisting vibration of the Ch_2 groups, and the stretching vibration of C–C bonds also created a peak at the Raman shift 1216 cm^{-1} (Jung et al. 2018). The peaks at Raman shifts 1327 cm^{-1} and 1358 cm^{-1} were associated with the twisting vibrations of CH_2 groups and the wagging vibrations of CH_3 groups, respectively (Rizzarelli et al. 2016). The peaks on Raman shifts 1433 cm^{-1} and 1457 cm^{-1} were also associated with the bending vibrations of the CH_2 group (Jung et al. 2018). It can be observed in the spectrums demonstrated in Fig. 2b that the same peaks were observed in the samples exposed to microbial strain B and control
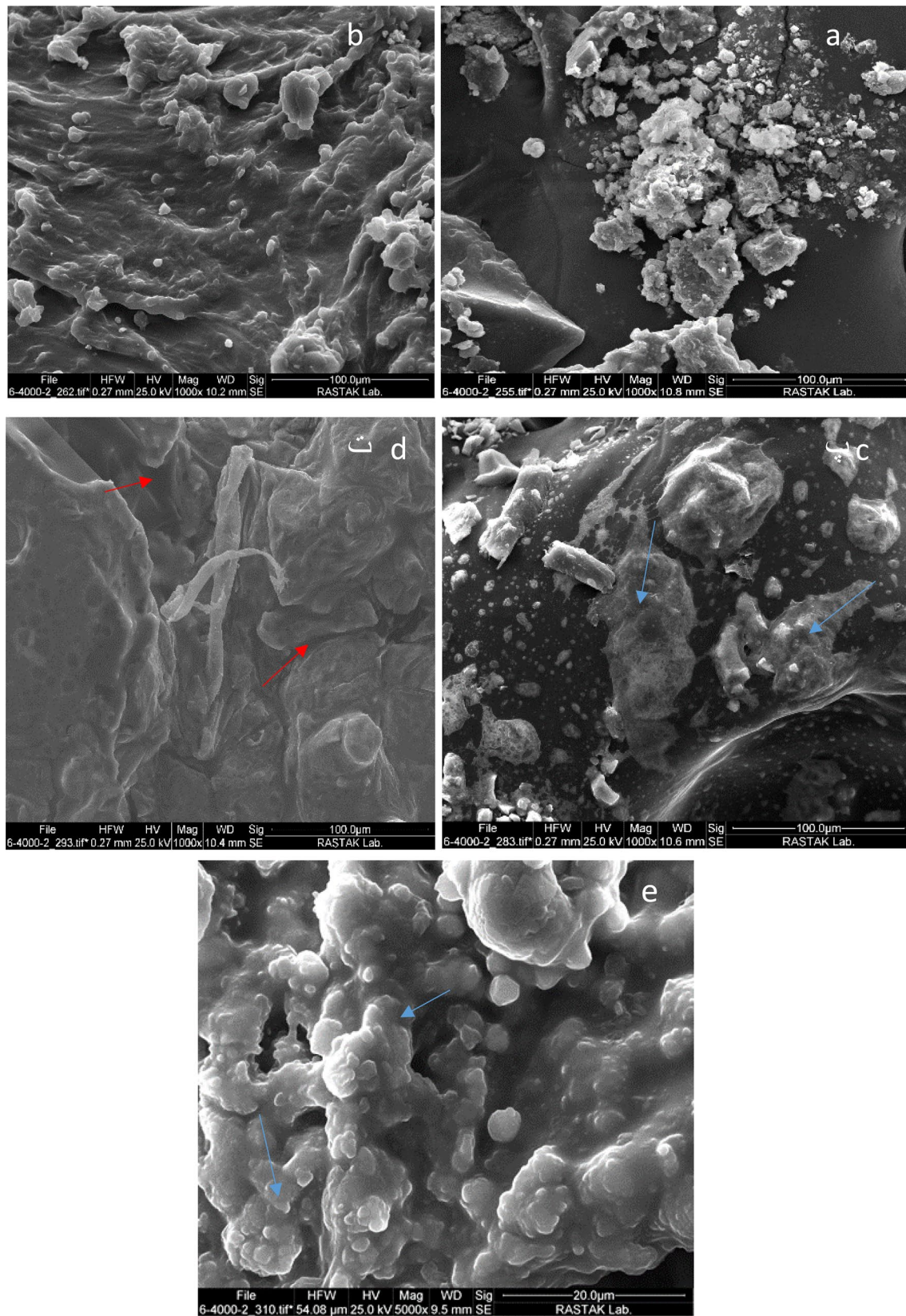
Fig. 1 The micrographs resulting from the SEM tests for samples **a** control PP, **b** control PE, **c** PP exposed to the microbial strain B, **d** PE exposed to the microbial strain C, and **e** PP exposed to microbial strain E for three months
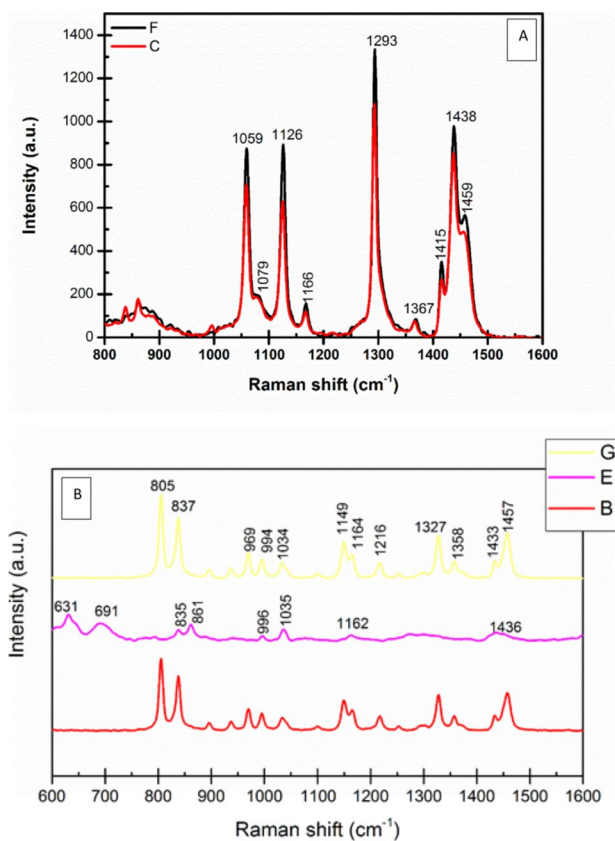
Fig. 2 a Raman spectrum of the PE base samples before (F) and after (C) exposure to bacterial strain C, **b** Raman spectrum of the PP base sample before (G) and after (B and E) exposure to B and E bacterial strains

Fig. 3 The FT-IR spectrums of samples based on **a** PP and **b** PE

samples, which indicates that the bacteria in this sample did not change the overall structure of the polypropylene polymer. In other words, the microbes in sample B only broke the polymer chain but failed to form a new structure and change the sample from its polypropylene state. Meanwhile, the samples exposed to microbial strain E indicated an entirely different Raman spectrum where some peaks were eliminated and replaced by new peaks in other Raman shifts. This reveals that the bacteria in this sample invaded the polymer chemical structure completely and formed new chemical structures. The peaks on Raman shifts 631 cm^{-1} and 691 cm^{-1} in this spectrum were associated with the bending vibrations of C–H bonds (Nielsen et al. 2002). Moreover, the peak on Raman shift 805 cm^{-1} was associated with the stretching vibrations of the C–C bonds, and the peak on Raman shift 837 cm^{-1} was associated with the rocking vibrations of CH$_3$ groups were moved to 835 cm^{-1} and 861 cm^{-1}, respectively, and the peaks on Raman shifts 969 cm^{-1}, 994 cm^{-1}, 1149 cm^{-1}, and 1433 cm^{-1} were moved to 996 cm^{-1}, 1035 cm^{-1}, 1162 cm^{-1}, and 1436 cm^{-1}, respectively, which indicates that these bonds were established in structure other than the PP polymer structure and reveals
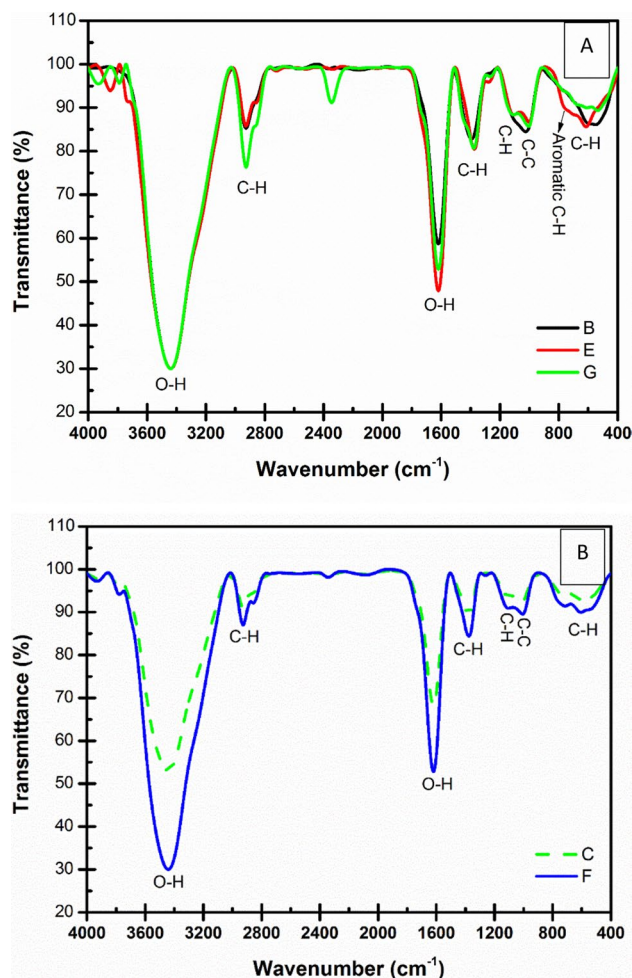
that the bacteria in this sample created chemical bonds with this polymer and impacted its chemical structure. Accurate determination of the new chemical structure resulting from the reaction between the bacteria and PP polymer requires further research.

Figure 3 demonstrates the spectrums resulting from the FT-IR tests for samples based on PE and PP.

In the FT-IR spectrum demonstrated in Fig. 3a which is from the polymers based on PP, there is a visible peak on wavenumber 3430 cm^{-1} which is associated with the stretching vibrations of the O–H bonds in the moisture adsorbed to the sample (Muthuselvi et al. 2018). The peak corresponding to the bending vibration of these O–H bonds is also observed at the wavenumber of around 16,601,149 cm^{-1}. The peaks observed at wavenumbers 2928 cm^{-1} and 2860 cm^{-1} were associated with the asymmetrical and symmetrical stretching vibrations of the C–H groups in the aliphatic structure of the pp polymer, respectively (Jung et al. 2018)). The peak observed at the wavenumber 2360 cm^{-1} corresponds to the CO$_2$ group resulting from the incomplete air evacuation

from the test container (Shahmoradi et al. 2020). The peaks observed on wavenumbers of around 1385 cm^{-1} and 1115 cm^{-1} were associated with the bending and wagging vibrations of the C–H bonds, respectively (Shahmoradi et al. 2020). The C–C bonds also indicated an adsorptive peak at 1010 cm^{-1}. Moreover, the peak observed at the wavenumber of around 640 cm^{-1} corresponds to the stretching vibration of the C–CH bonds (Shahmoradi et al. 2020). The presence of these peaks can confirm the presence of the PP structure in all three samples. Still, comparing the FT-IR spectrums of the three samples indicates that the peaks in samples exposed to microbial strains B and E went through significant changes compared to the control sample (G) which can be due to the PP polymer chains breaking in the presence of the microbes in these two samples. It can also be observed in sample E that the intensity of the peaks has changed and a new peak has emerged at wavenumber 758 cm^{-1} which was not present in the spectrums of samples B and G and indicates the presence of a new factor group in this sample. Given the complexities of analyzing the peaks present at low wavenumbers, the exact nature of the factor group associated with this peak must be determined through more precise tests, but the peak appears to be corresponding to the out-of-plane vibrations of the C–H bonds in an aromatic ring (Visentin et al. 2006). Thus, it appears the aromatic rings have formed on sample E in addition to the PP structure in this sample being invaded by the bacteria present in the sample. This change in structure appears to have changed the results of Raman and FT-IR tests.

The Ft-IR spectrums observed in Fig. 3b which are from the PE-based polymers indicated a peak observed at the wavenumber 3445 cm^{-1} which is associated with the stretching vibration of the O–H bonds in the moisture adsorbed to the sample (Motloung et al. 2016). The peak associated with the bending vibration of this bond was also observed at the wavenumber of around 1560 cm^{-1} (Shahmoradi et al. 2021). The peaks observed at wavenumbers or around 2930 cm^{-1} and 2855 cm^{-1} were also associated with the asymmetrical and symmetrical stretching vibrations of the C–H group present in the aliphatic structure of the polyethylene polymer (Visentin et al. 2006). The peaks observed at the wavenumbers of around 1374 cm^{-1} and 1121 cm^{-1} were associated with the bending and wagging vibrations of the C–H bonds, respectively (Visentin et al. 2006; Shahmoradi et al. 2021). The C–C bonds also demonstrated an absorptive peak at 1005 cm^{-1}. The peak observed at the wavenumber of around 600 cm^{-1} was also associated with the stretching vibration of the C–CH bonds (Visentin et al. 2006). A comparison of the two spectrums indicated that the intensity of the peaks declined in Sample C compared to the reference sample, but no new peak was observed and no peak was eliminated from the spectrum. This may indicate that despite the overall structural change in the polyethylene polymer

in the presence of the bacteria in the sample (as the results of TGA and Raman tests demonstrate), these bacteria have managed to break some of the carbon-hydrogen and carbon–carbon bonds in the PC structure along the polymer chains and make them shorter.

The thermal characteristics of the microplastics following exposure to the microbial strains were investigated using a TGA analysis. Figure 4 shows the TGA and DTG thermographs for PP and PE samples.

As shown in Fig. 4a, b, the TGA thermograph of sample G, in which the PP polymer was not exposed to microbes, only showed one weight loss at about 457 °C (Dong et al. 2009; Jung et al. 2010). The weight loss of the sample exposed to microbe B happened nearly at the same temperature, dropping from around 7.9 mg in sample G to about 4.5 mg. This implies that the microbe utilized in sample B did not alter the primary PP polymer structure but boosted its heat stability via complex formation. The Raman test findings confirmed the absence of PP polymer structural change caused by the microbe utilized in sample B.

The thermographs from sample E likewise show that the PP polymer structure was affected by the microbe in this sample, resulting in considerable alterations. Because of the absence of polar groups in its chemical structure, we know that the PP polymer is not hydrophilic, so no weight loss should be detected in the thermal range of water removal from the structure of this material (temperatures less than 200 °C). Nonetheless, sample E experienced weight loss in the temperature range of 50–150 °C (with the highest weight loss occurring around 97 °C), which was caused by the elimination of water adsorbed to the samples. The exposure of the PP polymer to microbes in sample E resulted in the production of polar groups in this sample, which formed hydrogen bonds with the water molecules present in the medium's moisture, resulting in water adsorption on the polymer's surface. The TGA analysis indicates that polar structures have developed on the PP polymer chains resulting from exposure to microbial strain E. In addition to the weight loss observed in this sample in the thermal range of 440–520 °C (with the maximum weight drop at 460 °C), which corresponded to the thermal decomposition of the intact PP polymer, another weight loss was observed in this sample in the 220–375 °C thermal range (with the maximum weight loss at 281 °C). This weight-loss phase might be caused by the heat degradation of the PP polymers broken by the microbes in this sample. The TGA test can not reveal the specific chemical structure of the products of the interaction between PP and this microbe, but the findings indicate that these compounds have poorer thermal stability than the PP polymer chain and, thus, decompose at lower temperatures.

According to similar studies, the TGA thermograph of sample F, in which the PE polymer was not exposed to any microbial strains, underwent only one weight loss at
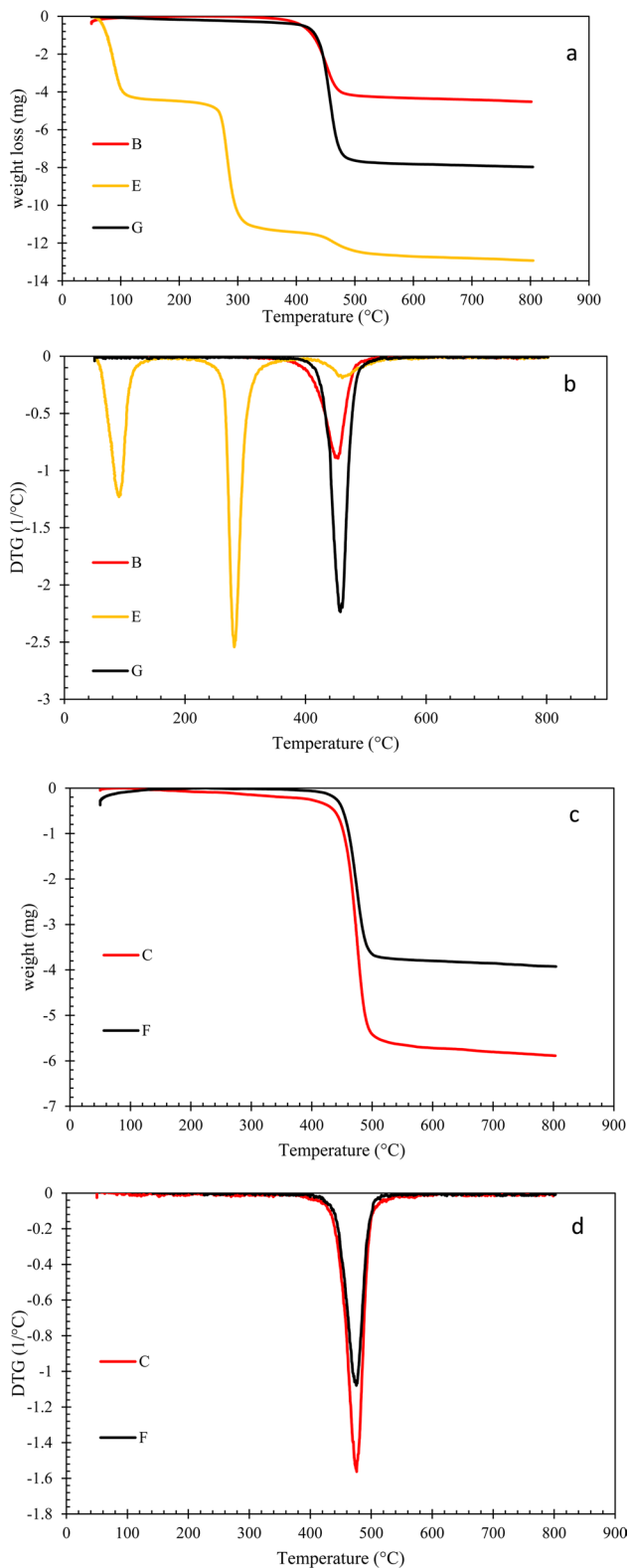
Fig. 4 TGA (**a**, **c**) and DTG (**b**, **d**) thermographs of samples of PP-based (**a**, **b**) and PE-based (**c**, **d**)

the range of 400–530 °C (with the maximum weight drop at 476 °C), which is due to the thermal decomposition of the polyethylene chain (Miandad et al. 2019; Kumar and Singh 2013). The thermograph of sample C shows a weight loss at about the same temperature as the control sample, but the quantity of weight loss varied from approximately 3.9 mg to around 5.9 mg in sample C. This result suggests that the microbe utilized in the sample did not alter the primary structure of the PE polymer but instead resulted in the formation of products with poorer thermal stability than PE polymer.

The mean weight loss of the PP samples subjected to bacterial strains B and E was 38.2% and 58.9%, respectively, according to the results of cellular gravity studies. The more considerable sample weight loss when exposed to microbial strain E compared to microbial strain B suggested that this strain had a more substantial influence on the decomposition of polypropylene-based microplastic chemical structure, as previously found in testing. Furthermore, the mean cellular gravity decrease for PE-based microplastic subjected to strain C was 13.3%, the lowest among the strains examined in this study. Furthermore, evaluating the generated carbon dioxide revealed that the average quantity of CO_2 was 3.76, 4.49, and 0.83 gr/l for samples exposed to strains B, E, and C, respectively. Evaluating isolate growth based on protein creation revealed that samples exposed to strains B, E, and C created an average of 4.86, 8.59, and 1.49 gr/l of protein, respectively. Thus, these findings support the findings of the cellular gravity test, indicating that strain E has a stronger influence on microplastic structure disintegration than the other two strains. Furthermore, while the sample subjected to strain C had microstructural changes in its surface, the spikes on the surface of the PE microplastic did not change considerably after exposure to this strain, and the surface remained relatively smooth. Thus, the findings of the three tests above corroborated the microscopic test results.

Conclusion

Untreated microplastics have been reported from 80 to 2000 particles per cubic meter. This number has been published in various reports that show from 1000 to 50,000 particles per cubic meter (Carr et al. 2016), but this amount has been reported with an efficiency of more than 98% in the collection from an urban house (Lares et al. 2018) which is reported with a number of 3500 Is. The particle per liter of wastewater does not match, which can be due to the low efficiency of the urban treatment plant system in south Tehran in removing these particles or the excessive number in the raw limit. Also, microplastics in the environment include a wide variety of sizes and materials (Kelly et al. 2021). The reason for this increase may be due to the variable size of

particles measured in different studies. In this study, particles more than 0.2 μm were evaluated and nanoplastics were 72. They made up 34% of it, so different results may be obtained if particles with different sizes are measured.

The relative abundance of particles showed that the highest amount was related to microfibers, followed by fragments. Microfibers are the most types of microplastics in the flow of raw sewage (McCormick et al. 2016) and they are the most common type (> 50%) in aquatic ecosystems as well (Moen et al. 2016). The amount of PP was the highest and the amount of PE ranked second in terms of the number of microplastics in the wastewater, which goes back to the source of production of these materials. In future research, the amount of these sources can be theoretically predicted and compared in reality (Conley et al. 2019). From all the tests, we can conclude that firstly, bacterial strain *Pseudomonas aestusnigri* managed to leave the greatest impact on PP-based microplastic decomposition by changing the polymer structure, and secondly, although strains B and C did not change the chemical structure of PP and PE polymers, they intensified the decomposition of these microplastics which was more tangible in strain *Achromobacter denitrificans* than strain *Bacillus amyloliquefaciens*.

Declarations

Conflict of interest The authors declare that they have no conflict of interest.

Ethical approval This study was approved by the authors.

References

Auta HS, Emenike C, Fauziah S (2017) Distribution and importance of microplastics in the marine environment: a review of the sources, fate, effects, and potential solutions. Environ Int 102:165–176. https://doi.org/10.1016/J.ENVINT.2017.02.013

Bräutigam S, Dennewald D, Schürmann M, Lutje-Spelberg J, Pitner W-R, Weuster-Botz D (2009) Whole-cell biocatalysis: evaluation of new hydrophobic ionic liquids for efficient asymmetric reduction of prochiral ketones. Enzyme Microb Technol 45:310–316. https://doi.org/10.1016/J.ENZMICTEC.2009.06.015

Burns EE, Boxall ABA (2018) Microplastics in the aquatic environment: evidence for or against adverse impacts and major knowledge gaps. Environ Toxicol Chem 37:2776–2796. https://doi.org/10.1002/etc.4268

Carr SA, Liu J, Tesoro AG (2016) Transport and fate of microplastic particles in wastewater treatment plants. Water Res 91:174–182. https://doi.org/10.1016/j.watres.2016.01.002

Cerqueira MA, Souza BWS, Teixeira JA, Vicente AA (2013) Utilization of galactomannan from *Gleditsia triacanthos* in polysaccharide-based films: effects of interactions between film constituents on film properties, food and bioprocess. Technology 6:1600–1608. https://doi.org/10.1007/s11947-011-0753-x

Chen G-Q, Patel MK (2012) Plastics derived from biological sources: present and future: a technical and environmental review. Chem Rev 112:2082–2099. https://doi.org/10.1021/cr200162d

Conley K, Clum A, Deepe J, Lane H, Beckingham B (2019) Wastewater treatment plants as a source of microplastics to an urban estuary: removal efficiencies and loading per capita over one year. Water Res X 3:100030. https://doi.org/10.1016/j.wroa.2019.100030

Dong Q, Kumada N, Yonesaki Y, Takei T, Kinomura N (2009) Hydrothermal synthesis of Fe_3O_4 particles with various shapes. J Ceram Soc Jpn 117:881–886. https://doi.org/10.2109/jcersj2.117.881

Elahi A, Bukhari DA, Shamim S, Rehman A (2021) Plastics degradation by microbes: a sustainable approach. J King Saud Univ Sci 33:101538. https://doi.org/10.1016/J.JKSUS.2021.101538

Fukuda H, Hama S, Tamalampudi S, Noda H (2008) Whole-cell biocatalysts for biodiesel fuel production. Trends Biotechnol 26:668–673. https://doi.org/10.1016/J.TIBTECH.2008.08.001

Furukawa T, Sato H, Kita Y, Matsukawa K, Yamaguchi H, Ochiai S et al (2006) Molecular structure, crystallinity and morphology of polyethylene/polypropylene blends studied by Raman mapping, scanning electron microscopy, wide angle X-ray diffraction, and differential scanning calorimetry. Polym J 38:1127–1136. https://doi.org/10.1295/polymj.PJ2006056

Gao R, Sun C (2021) A marine bacterial community capable of degrading poly(ethylene terephthalate) and polyethylene. J Hazard Mater 416:125928. https://doi.org/10.1016/J.JHAZMAT.2021.125928

Halden RU (2010) Plastics and health risks. Annu Rev Public Health 31:179–194. https://doi.org/10.1146/annurev.publhealth.012809.103714

Horton AA, Dixon SJ (2018) Microplastics: an introduction to environmental transport processes. Wires Water 5:e1268. https://doi.org/10.1002/wat2.1268

Issac MN, Kandasubramanian B (2021) Effect of microplastics in water and aquatic systems. Environ Sci Pollut Res 28:19544–19562. https://doi.org/10.1007/s11356-021-13184-2

Jung S-H, Cho M-H, Kang B-S, Kim J-S (2010) Pyrolysis of a fraction of waste polypropylene and polyethylene for the recovery of BTX aromatics using a fluidized bed reactor. Fuel Process Technol 3:277–284. https://doi.org/10.1016/J.FUPROC.2009.10.009

Jung MR, Horgen FD, Orski SV, Rodriguez V, Beers KL, Balazs GH et al (2018) Validation of ATR FT-IR to identify polymers of

plastic marine debris, including those ingested by marine organisms. Mar Pollut Bull 127:704–716. https://doi.org/10.1016/j.marpolbul.2017.12.061

Kelly JJ, London MG, McCormick AR, Rojas M, Scott JW, Hoellein TJ (2021) Wastewater treatment alters microbial colonization of microplastics. PLoS ONE 16(1):e0244443. https://doi.org/10.1371/journal.pone.0244443

Kumar S, Singh RK (2013) Thermolysis of high-density polyethylene to petroleum products. J Pet Eng 2013:1–7. https://doi.org/10.1155/2013/987568

Lares M, Ncibi MC, Sillanpaa M, Sillanpaa M (2018) Occurrence, identification and removal of microplastic particles and fibers in conventional activated sludge process and advanced MBR technology. Water Res 133:236–246. https://doi.org/10.1016/j.watres.2018.01.049

Lowry O, Rosebrough N, Farr AL, Randall R (1951) Protein measurement with the Folin phenol reagent. J Biol Chem 193:265–275. https://doi.org/10.1016/S0021-9258(19)52451-6

McCormick AR, Hoellein TJ, London MG, Hittie J, Scott JW, Kelly JJ (2016) Microplastic in surface waters of urban rivers: concentration, sources, and associated bacterial assemblages. Ecosphere 7:e01556. https://doi.org/10.1002/ecs2.1556

Miandad R, Rehan M, Barakat MA, Aburiazaiza AS, Khan H, Ismail IMI et al (2019) Catalytic pyrolysis of plastic waste: moving toward pyrolysis based biorefineries. Front Energy Res 7:27. https://doi.org/10.3389/FENRG.2019.00027

Moen B, Røssvoll E, Måge I, Møretrø T, Langsrud S (2016) Microbiota formed on attached stainless steel coupons correlates with the natural biofilm of the sink surface in domestic kitchens. Can J Microbiol 62:148–160. https://doi.org/10.1139/cjm-2015-0562

Motloung SV, Tsega M, Dejene FB, Swart HC, Ntwaeaborwa OM, Koao LF et al (2016) Effect of annealing temperature on structural and optical properties of $ZnAl_0O_4$:1.5% Pb2+ nanocrystals synthesized via sol–gel reaction. J Alloys Compd 677:72–79. https://doi.org/10.1016/j.jallcom.2016.03.170

Muthuselvi C, Pandiaraja SS, Ravikumar B, Athimoolam S, Srinivasan N, Krishnakum RV (2018) FT-IR and FT-Raman spectroscopic analyzes of Indeno quinoxaline derivative crystal. Asian J Appl Sci 11:83–91. https://doi.org/10.3923/ajaps.2018.83.91

N. Marine Debris Program, Detecting Japan Tsunami Marine Debris at Sea: A Synthesis of Efforts and Lessons Learned Acknowledgements Contents, 2015. https://marinedebris.noaa.gov/sites/default/files/JTMD_Detection_Report.pdf. Accessed 2 May 2022

Nielsen A, Batchelder D, Pyrz R (2002) Estimation of crystallinity of isotactic polypropylene using Raman spectroscopy. Polymer 43:2671–2676. https://doi.org/10.1016/S0032-3861(02)00053-8

North EJ, Halden RU (2013) Plastics and environmental health: the road ahead. Rev Environ Health 28:1–8. https://doi.org/10.1515/reveh-2012-0030

Prata JC (2018) Microplastics in wastewater: state of the knowledge on sources, fate and solutions. Mar Pollut Bull 129:262–265. https://doi.org/10.1016/J.MARPOLBUL.2018.02.046

Rizzarelli P, Rapisarda M, Perna S, Mirabella EF, La Carta S, Puglisi C et al (2016) Determination of polyethylene in biodegradable polymer blends and in compostable carrier bags by Py-GC/MS and TGA. J Anal Appl Pyrolysis 117:72–81. https://doi.org/10.1016/j.jaap.2015.12.014

Sambrook J, Russell DW (2006) Isolation of high-molecular-weight DNA from mammalian cells using formamide. CSH Protoc 2006:3225. https://doi.org/10.1101/pdb.prot3225

Shahmoradi AR, Talebibahmanbigloo N, Javidparvar AA, Bahlakeh G, Ramezanzadeh B (2020) Studying the adsorption/inhibition impact of the cellulose and lignin compounds extracted from agricultural waste on the mild steel corrosion in HCl solution. J Mol Liq 304:112751. https://doi.org/10.1016/j.molliq.2020.112751

Shahmoradi AR, Talebibahmanbigloo N, Nickhil C, Nisha R, Javidparvar AA, Ghahremani P et al (2021) Molecular-MD/atomic-DFT theoretical and experimental studies on the quince seed extract corrosion inhibition performance on the acidic-solution attack of mild-steel. J Mol Liq 346:117921. https://doi.org/10.1016/J.MOLLIQ.2021.117921

Susanti NKY, Mardiastuti A, Wardiatno Y (2020) Microplastics and the impact of plastic on wildlife: a literature review. IOP Conf Ser Earth Environ Sci 528:012013. https://doi.org/10.1088/1755-1315/528/1/012013

Visentin M, Stea S, De Clerico M, Reggiani M, Fagnano C, Squarzoni S et al (2006) Determination of crystallinity and crystal structure of Hylamer polyethylene after in vivo wear. J Biomater Appl 21:131–145. https://doi.org/10.1177/0885328206058786

Yoshida S, Hiraga K, Takehana T, Taniguchi I, Yamaji H, Maeda Y et al (2016) A bacterium that degrades and assimilates poly(ethylene terephthalate). Science 351:1196–1199. https://doi.org/10.1126/science.aad6359

Żwierełło W, Maruszewska A, Skórka-Majewicz M, Goschorska M, Baranowska-Bosiacka I, Dec K et al (2020) The influence of polyphenols on metabolic disorders caused by compounds released from plastics. Rev Chemosphere 240:124901. https://doi.org/10.1016/J.CHEMOSPHERE.2019.124901